Magnetic diagnostics using the third-harmonic magnetic response for a molecule-based magnet networked by a single chiral ligand

M. Mito,[1,a)] K. Iriguchi,[1] H. Deguchi,[1] J. Kishine,[1,b)] Y. Yoshida,[2] and K. Inoue[2]
[1]*Faculty of Engineering, Kyushu Institute of Technology, Kitakyushu, 804-8550, Japan*
[2]*Department of Chemistry and Institute for Advanced Materials Research, Hiroshima University, Higashihiroshima 739-8526, Japan*

(Received 5 January 2012; accepted 28 April 2012; published online 30 May 2012; publisher error corrected 4 June 2012)

We investigated complex magnetic domain formation on a chiral molecule-based magnet, $[Cr(CN)_6][Mn(R)\text{-}pnH(H_2O)](H_2O)$ (termed as *R*-GN), whose two-dimensional molecular network was constructed with the help of a single-handed chiral ligand ((*R*)-pn). There, the first- and third-harmonic magnetic responses ($M_{1\omega}$ and $M_{3\omega}$) against the ac magnetic field were observed, and magnetic hysteresis in ac field of a few Oe was discussed in terms of Rayleigh loop. The diagnostics of this magnetic hysteresis clarified the complex process of magnetic domain formation against a change in temperature. For *R*-GN, it was reported that a giant $M_{3\omega}$ (termed **#4** in this paper) appeared just above the so-called "magnetic ordering temperature (T_C)." In the present study, three $M_{3\omega}$ responses (**#1-3**) were newly observed on the lower-temperature side of **#4**, and the ac field dependencies for all of **#1-#4** were investigated. **#1** also accompanied the giant $M_{3\omega}$, which suggests that a significant degree of magnetic fluctuation surviving below T_C. This glassy behavior below T_C is an attractive new phenomenon in molecule-based magnets with a single-handed chiral ligand. **#2** and **#3** exhibited magnetic ordering and the formation of a small magnetic domain, respectively. The $M_{3\omega}$ responses of **#1-3** were suppressed with increasing the amplitude of ac field, and the corresponding magnetic hysteresis was a normal Rayleigh loop accompanying the out-of-phase of the $M_{1\omega}$ response. The $M_{3\omega}$ response of **#4** without the out-of-phase of $M_{1\omega}$ was, however, enhanced with increasing the amplitude of ac field, and **#4** represented a large magnetic hysteresis in the paramagnetic region, intrinsically different from those of **#1**-**#3**. © *2012 American Institute of Physics*. [http://dx.doi.org/10.1063/1.4721806]

I. INTRODUCTION

Crystallographically, "chirality" requires any polar crystal structure that does not have an inversion center and, in that medium, the spatial reversal symmetry of crystal structure is broken. A strategy for the creation of a structurally chiral magnet is a chemical approach relying upon a spontaneous resolution process using proper bridging ligands.[1] In the Prussian-Blue family of molecule-based magnets, the intentional construction of crystallographic chirality with high dimensionality, using the association of a chiral organic ligand, has been successfully performed.[2,3] If the target material could have large spontaneous magnetic moments accompanying the breaking of the time reversal symmetry, the magnetic second-harmonic generation (MSHG)[4–6] and the magneto-chiral dichroism (MChD) effects[7–10] would be quite promising for industrial applications. MSHG has been observed in a ferromagnetic material that has electric polarization, and it detects broken inversion symmetry in the electric dipole, coupled with spontaneous magnetization. Thus, MSHG depends on magnetically ordered symmetry, leading to the detection of antiferromagnetic domains[11] and photographs of it.[12] The microscopic origin of MSHG is considered to be mainly due to the interaction of the spin-orbit coupling through the electric-dipole nonlinearity that is allowed by broken inversion symmetry of crystal structure.[13]

The present study reveals that in a structurally chiral molecule-based ferrimagnet, the nonlinear magnetic susceptibility as a function of the frequency (f) and amplitude (h) of the ac field, as well as temperature (T), is effective for the study of magnetic domain formation, as in the case of the MSHG measurement. By analyzing the complex harmonic responses obtained there, we can understand the magnetic hysteresis in the low magnetic field region, and we can address the variations in magnetic domain formation against the change in T. Prior to describing the experimental data, we will first review the nonlinear magnetic response in an ac magnetic field, and then introduce the targeted material.

II. NONLINEAR MAGNETIC RESPONSES

The magnetic moment reflects not only the spin of primary elements such as magnetic ions, atoms, molecules, etc., but also their many-body effects. When a magnet is placed under an oscillating field (ac field) of $H_{AC} = h \cos \omega t$, the time dependence of the magnetization, $M(t)$, is usually expressed as follows:

$$M(t) = M_{1\omega} \cos \omega t + M_{2\omega} \cos 2\omega t + M_{3\omega} \cos 3\omega t + \ldots, \quad (1)$$

where ω ($=2\pi f$, f is the frequency of H_{AC}) is the angular frequency and $M_{n\omega}$ (n: integer) represents the nth-harmonic

a)Author to whom correspondence should be addressed. Electronic mail: mitoh@tobata.isc.kyutech.ac.jp. Tel./FAX: 81-93-884-3286.
b)Present address: Graduate School of Arts and Sciences, The Open University of Japan, Chiba 261-8586, Japan.

magnetic response. In an actual system, there is often a time delay in the response to H_{AC}, which results in the appearance of an out-of-phase component. These detailed analyses of higher-order harmonic responses ($M_{n\omega}$, $n \geq 2$) as well as of the first one ($M_{1\omega}$), as a function of f, h, and T, elucidate the process of magnetic domain formation in the warming or cooling process: In small h, $M_{2\omega}$ is connected to the breaking of the time inversion symmetry, and the large signal reflects the presence of spontaneous magnetization. On the other hand, $M_{3\omega}$ is connected to the microscopic breaking of spatial symmetry of magnetic moment, and the anomaly confirms the presence of magnetic domain formation, which manifests a long-range magnetic order (accompanying the large phase change), for example, or a glassy state (that does not accompany the large phase change).[14–17] There have been successful studies using $M_{3\omega}$ on the magnetic domain in ferromagnetic materials.[18,19] The study of a magnetic glass-state using $M_{3\omega}$ plus $M_{2\omega}$ has also been successfully conducted upon triangular antiferromagnets[20] and networked single molecule magnets.[21] Thus, such a study of magnetic property using $M_{3\omega}$ is quite effective for the elucidation of magnetic transformation, i.e., from paramagnetic to ordered states, in complex magnetic matter.

On the other hand, this $M_{3\omega}$ response is also useful for the investigation of magnetic hysteresis in a small ac magnetic field. A fundamental study of the domain wall (DW) under an ac field was conducted by Rayleigh at the end of the 19th century.[22] When a small magnetic field $\boldsymbol{H}$ is applied, domains parallel to $\boldsymbol{H}$ grow. In this process, the DWs move, and their moving is sometimes hindered by material defects. Rayleigh studied this phenomenon, and quantified the magnetization M as being the sum of the linear and quadratic terms in the field.[22–25] When H showing cyclic change is replaced with the ac field, $M(t)$ is represented as the sum of the first harmonic component ($M_{1\omega}$ term) with a loss term, namely, a delay in phase, and the third-harmonic component ($M_{3\omega}$ term).[22–26] This phenomenon reflects discontinuous displacements of the DWs in a series of potential wells, which of course accompany the energy loss.[27] Thus, the presence of $M_{3\omega}$ also reveals whether or not magnetic hysteresis appears prominently in a given situation. In a few typical ferromagnets such as Gd,[24,26] Tb,[26] Dy,[28] and Ni,[25] low-field magnetic hysteresis below the magnetic ordering temperature (T_C) has been well explained via the $M_{1\omega}+M_{3\omega}$ response in the sense of the Rayleigh law. Recently, in Dy, many anomalies in $M_{3\omega}$ were connected with the spin-locking phenomenon, reflecting a slight change in the magnetic hysteresis as a function of T.[28] Thus, we can acquire important knowledge on magnetic domain formation at the low field limit that cannot be obtained via the magnetic hysteresis in the large dc magnetic field. However, there has been no prototype of a study of magnetic hysteresis using the $M_{3\omega}$ response as applied to unique materials that exhibit complex magnetic behavior. In this paper, we carry out the diagnostics of magnetic hysteresis upon a molecule-based ferrimagnet with structural chirality, using $M_{3\omega}$.

III. TARGETED CHIRAL MOLECULE-BASED FERRIMAGNET

In the field of chemical synthesis, "chirality" is often indicated by the terms *R*-style or *S*-style. The present target compound is $[Cr(CN)_6][Mn(R)\text{-}pnH(H_2O)](H_2O)$ (termed an *R*-style green needle, *R*-GN),[3] which is a prototype of a "structurally chiral magnet" with a high-dimension molecular network.[1] (*R*)-pn represents an *R*-type of chiral ligand, (*R*)-1,2-diaminopropane, and is attached to an Mn^{2+} ion via the nitrogen atom of the (*R*)-pn itself. *R*-GN is a bimetallic ferrimagnet with a total spin of 5/2 $(Mn^{2+}) - 3/2$ $(Cr^{3+}) = 1$.[3] Crystallographically, this system belongs to the orthorhombic chiral space group $P2_12_12_1$. A two-fold helical axis is present along each principal crystal axis. Independent of the chirality of the organic ligand, green needle-like single crystals of all styles were obtained, such as the *R*-, *S*-, and racemic styles, and we have termed these crystals "GN." There is no distinct difference in the crystal structure and magnetic property between *R*-GN and *S*-GN, except for the chirality of 1,2-diaminopropane. In the racemic system (*rac*-GN), where equal percentages of *R*-pn and *S*-pn are mixed in the process of synthesis, the space group is $P2_1/m$, where the structural chirality is lost.[29] *R*(*S*)-GN exhibits magnetic ordering near 37 K (the present study will reveal that the precise T_C is lower than 37 K), and it is a soft magnet with a saturation field of about 30 Oe.[3]

It has already been reported that a giant $M_{3\omega}$ response appears in *R*-GN slightly above T_C.[30] This response has not been observed in *rac*-GN. In this paper, we term this "response **#4**." Here, we report that on a much lower temperature side than T_C, another giant $M_{3\omega}$ response (response **#1**) appears, and it exhibits *f*- and *h*-dependencies that are considerably different from those of **#4**. Furthermore, two additional responses, **#2** and **#3**, are observed near T_C. By investigating these diverse $M_{3\omega}$ responses, in terms of their *f*- and *h*-dependencies, the details of the complex magnetic domain formation in *R*-GN are elucidated.

IV. EXPERIMENTAL PROCEDURE

AC magnetic susceptibility measurements were carried out using a superconducting quantum interference device (SQUID) magnetometer (Quantum Design, MPMS). This was used to obtain the time dependence of magnetization, $M(t)$, and the amplitude of $M(t)$ and its time delay against H_{AC} for each harmonic component were then independently evaluated. They were also evaluated in terms of the style of the in-phase and out-of-phase components. The residual dc field (H_r) was carefully reduced to less than 1% of the earth field in order to evaluate the small magnetic hysteresis at the zero dc field limit. The magnetic hysteresis mentioned hereafter represents the hysteresis in the ac magnetic field.

In *R*-GN, the *a*-axis is the magnetic easy axis.[3] A series of ac harmonic responses has been measured at $\boldsymbol{H}_{AC}$ parallel to each principle axis,[30] and a prominent $M_{n\omega}$ ($n \geq 2$) was observed only for $\boldsymbol{H}_{AC} // \boldsymbol{a}$. For $\boldsymbol{H}_{AC} // \boldsymbol{b}$, $\boldsymbol{c}$, the magnitude of $M_{n\omega}$ ($n \geq 2$) was below a level of being able to do a meaningful discussion about the *h*- and *f*-dependencies. Therefore, the *h*- and *f*-dependencies are presented only for

$\boldsymbol{H}_{AC}//\boldsymbol{a}$. The series of results presented here was obtained through three runs. Those of the first and second runs are shown in Figs. 2 and 1, respectively, and those of the third run are shown in Figs. 3 and 4. The mass of the large single crystal used in the first run was 0.70 mg. We could not measure the confident mass for the crystal used in the second and third runs, and as a result, we evaluated the magnetic response in Figs. 1, 3, 4, 6, and 7, which were obtained via the second and third runs, in terms of emu units. A series of magnetic anomalies was labeled by increasing the number from the low-temperature side. The detection accuracy of $M_{3\omega}$ depends on the intensity of power noise, which is intermixed to the intrinsic magnetic response.

V. EXPERIMENTAL RESULTS

We now describe the experimental results for the $M_{1\omega}$ and $M_{3\omega}$ responses of *R*-GN at $\boldsymbol{H}_{AC}//\boldsymbol{a}$, as obtained over a wider temperature range in terms of (1) the *h*-dependence at $f = 1$ Hz (Fig. 1), (2) the *f*-dependence at $h = 2.0$ Oe (Fig. 2, the results have already been presented in part in Ref. 30), and (3) the *f*-dependence at $h = 0.1$ Oe (Figs. 3 and 4).

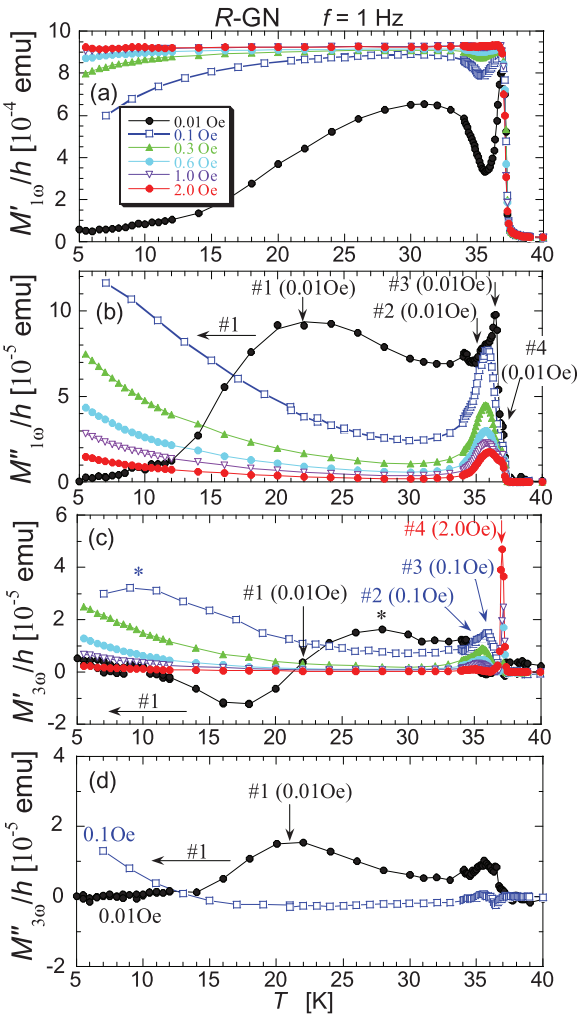

FIG. 1. In-phase $M'_{1\omega}(T)/h$ (a) and out-of-phase $M''_{1\omega}(T)/h$ (b) components of the 1ω magnetic response, and in-phase $M'_{3\omega}(T)/h$ (c) and out-of-phase $M''_{3\omega}(T)/h$ (d) components of the 3ω magnetic response for *R*-GN at H_{AC} of $f = 1$ Hz for $0.01 \le h \le 2.0$ Oe. In (d), the data for $M''_{3\omega}(T)/h$ for $h \ge 0.3$ Oe were omitted because of their negligible magnitude. In (c), the shift in $M'_{3\omega}(T)/h$ can be tracked by following the temperature of the characteristic peak (marked with *). The ac field was applied in a direction parallel to the *a*-axis. This figure can essentially be compared with Fig. 4 of Ref. 30, as it presents only the *h*-dependence of **#4**, and provides an extension of the temperature range and an exploration at lower amplitude.

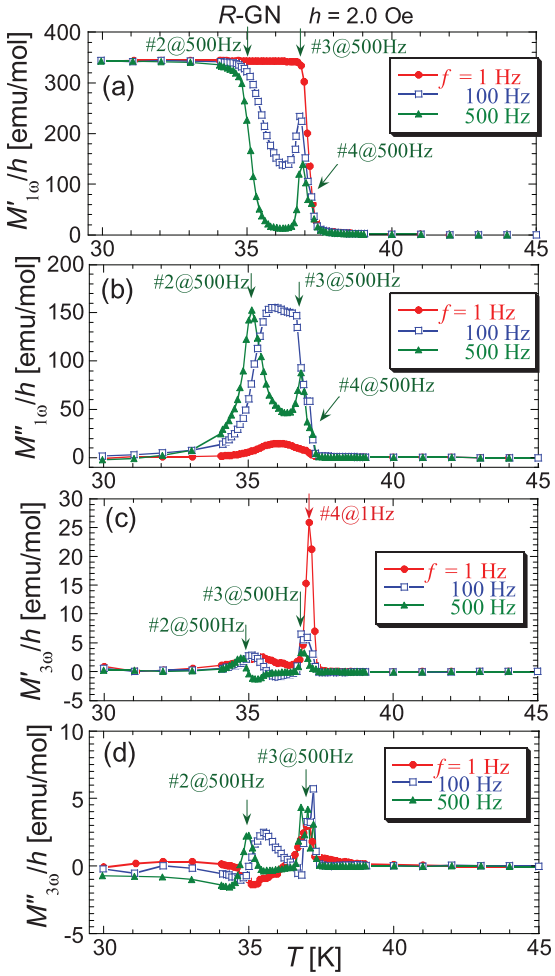

FIG. 2. In-phase $M'_{1\omega}(T)/h$ (a) and out-of-phase $M''_{1\omega}(T)/h$ (b) components of the 1ω response and in-phase $M'_{3\omega}(T)/h$ (c) and out-of-phase $M''_{3\omega}(T)/h$ (d) components of the 3ω magnetic response for *R*-GN at $H_{AC}(h = 2.0$ Oe) for $f = 1$, 100, and 500 Hz. The ac field was applied in a direction parallel to the *a*-axis. The data in (a)-(c) have already been presented in Ref. 30, but it is important to present them here in order to distinguish among the four kinds of magnetic anomalies.

Figure 1 shows the in-phase and out-of-phase components of both $M_{1\omega}/h$ ($M'_{1\omega}(T)/h$ and $M''_{1\omega}(T)/h$) and $M_{3\omega}/h$ ($M'_{3\omega}(T)/h$ and $M''_{3\omega}(T)/h$) responses for *R*-GN as a function of *T* at $H_{AC}(f = 1.0$ Hz) for $h = 0.01$-2.0 Oe. As shown in Fig. 1(a), for $h \le 0.3$ Oe, a prominent splitting of magnetic anomalies at 30–37 K was observed. For $h \ge 0.6$ Oe, however, the confirmation of several anomalies at $f = 1$ Hz is difficult if we look only at the data of $M'_{1\omega}(T)/h$. The above-mentioned anomalies can, however, be distinctly recognized in the temperature dependence of $M'_{3\omega}(T)/h$ (Fig. 1(c)). Here, the negative value of $M'_{3\omega}$ means that the phase delay against the ac field is more than $\pi/2$ rad. By focusing $M'_{3\omega}(T)/h$ near 35–36 K at $f = 1$ Hz, we see that this broad hump indeed consists of two anomalies. Here, these responses are termed **#2** and **#3** from the low-temperature side, respectively. A detailed explanation of this phenomenon is offered in the description in Figs. 2, 3, and 4. Below, we emphasize the fact that on the

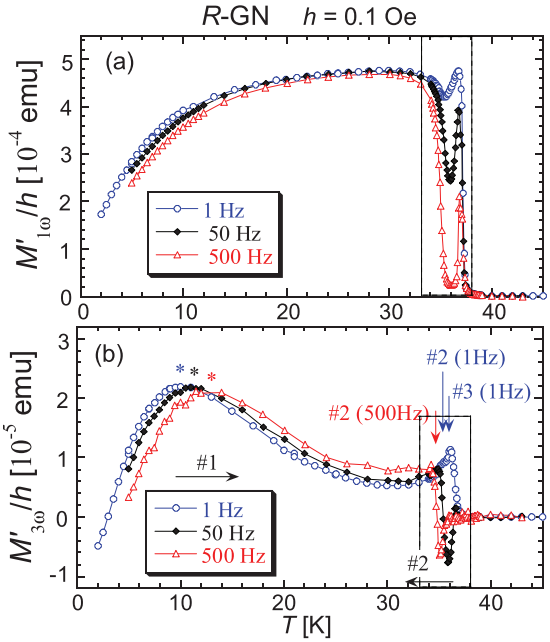

FIG. 3. $M'_{1\omega}(T)/h$ (a) and $M'_{3\omega}(T)/h$ (b) for *R*-GN at H_{AC} for $f = 1$, 50, and 500 Hz. The amplitude of the ac field (h) was 0.1 Oe. The ac field was applied in a direction parallel to the *a*-axis. For the vertical rectangular region enclosed by solid lines in each figure, more detailed data are shown in Fig. 4. Figure 3 complements the data of Fig. 1 at $h = 0.1$ Oe towards lower temperatures, and the frequency dependencies of $M'_{1\omega}(T)/h$ (a) and $M'_{3\omega}(T)/h$ (b) are presented so that the frequency dependencies of **#1**-**#3** can be observed.

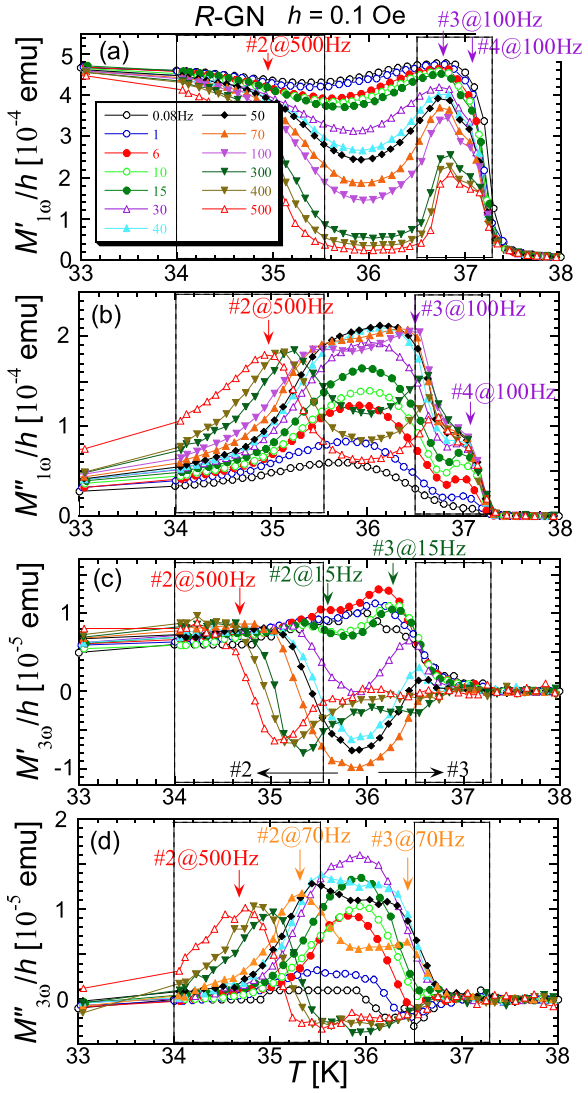

FIG. 4. Frequency dependencies of $M'_{1\omega}(T)/h$ (a), $M''_{1\omega}(T)/h$ (b), $M'_{3\omega}(T)/h$ (c), $M''_{3\omega}(T)/h$ (d) for *R*-GN in the temperature range of 33-38 K. The amplitude of the ac field (h) was 0.1 Oe. Note: some squares serve only to guide the eye so that the shift in each anomaly can be observed. This figure is comparable with Fig. 3 of Ref. 30, which shows the frequency dependence of each response at $h = 2$ Oe.

lower-temperature side of these anomalies, there is one magnetic anomaly with a large $M_{3\omega}$ response, which was observed only at a small h. This new anomaly is labeled as **#1**. This **#1** response accompanies the anomaly of $M''_{1\omega}(T)/h$ (see Fig. 1(b)), which suggests that the phenomenon is accompanied by energy loss, and it becomes dominant with decreasing h. Moreover with increasing h, the $M_{3\omega}$ response for **#1** shifted considerably toward the low-temperature side (see Fig. 1(c)). The chiral ligand is known to have a prominent electric dipole. Here, we presume that the presence of nonequivalent magnetic sites owing to the chiral ligand causes any fluctuation in the magnetic moments, with the result that the magnetic fluctuation survives in the case of small h, even for $T < T_C$. We should also mention that it has already been reported that there is a large $M_{3\omega}$ response, termed **#4**, on the high-temperature side of **#3**, which increases with increasing h and exceeds 10% of $M_{1\omega}$ at $h \geq 4$ Oe.[30] In this regard, we stress that the $M_{3\omega}$ response for **#1** at small h is comparable to that for **#4** at large h.

Figure 2 shows the temperature dependencies of the in-phase and out-of-phase components of both $M_{1\omega}/h$ and $M_{3\omega}/h$ against H_{AC} of $h = 2.0$ Oe for $f = 1$, 100, and 500 Hz in the temperature range of 30-45 K. (The data for 30-40 K in (a)-(c) are consistent with Fig. 3 in Ref. 30.) As can be seen in Fig. 2(a), the splitting of $M'_{1\omega}/h$ becomes more prominent with increasing frequency. At $f = 500$ Hz, a first glance gives the impression that double anomalies exists at 35 K and 37 K; this splitting of $M'_{1\omega}/h$ with an increase in frequency indeed accompanies the enhancement of out-of-phase components (see Fig. 2(b)) for 34 K $< T <$ 37 K. Here, the low-frequency response at $h = 2.0$ Oe for 35 and 37 K is a response that is not accompanied by energy loss, while it is transformed into a response that is accompanied by energy loss with increasing frequency. Careful scrutiny of $M''_{1\omega}(T)/h$ for $f = 100$ and 500 Hz in Fig. 2(b) reveals that the anomaly at around 37 K actually consists of two anomalies: at 36.8 K (**#3**) and 37.1 K (**#4**). As can be seen in Fig. 2(c), **#4** presents huge $M'_{3\omega}$ at $f = 1$ Hz, while its magnitude is suppressed with increasing f. Figure 2(d) shows that **#4** is not accompanied by a phase delay against H_{AC}. In the ac magnetic measurement obtained under hydrostatic pressure using a polycrystalline sample[31] and under uniaxial strain using a single crystal,[32] the anomaly of $M'_{3\omega}/h$ due to **#4** was suppressed by the slight stress, and it disappeared under a stress corresponding to 7 kbar. On the other hand, that due to **#3** survives even at further pressure. A stress induces the structural defect as well as the lattice shrinkage. **#4** is the magnetic response appearing in the paramagnetic region, and its appearance requires structural

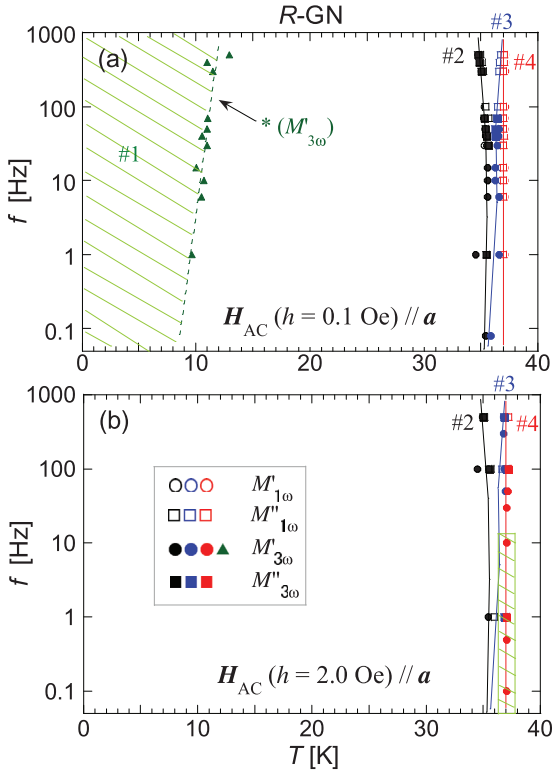

FIG. 5. Diagrams of temperature T vs. frequency f for R-GN at $\boldsymbol{H}_{AC}//\boldsymbol{a}$ with $h=0.1$ Oe and 2.0 Oe. The green area represents the region in which a giant $M_{3\omega}$ accompanying $M_{3\omega}/M_{1\omega}$ of more than 10% was observed. Due to the choice of temperature scale, the evolution of the different signals is not so easy to read. Solid and broken lines improve its readability.

uniformity over the entire crystal, which is more than that required for the other response.

The frequency dependencies of $M'_{1\omega}(T)/h$, $M''_{1\omega}(T)/h$, $M'_{3\omega}(T)/h$, and $M''_{3\omega}(T)/h$ at $h=0.1$ Oe are shown in Figs. 3

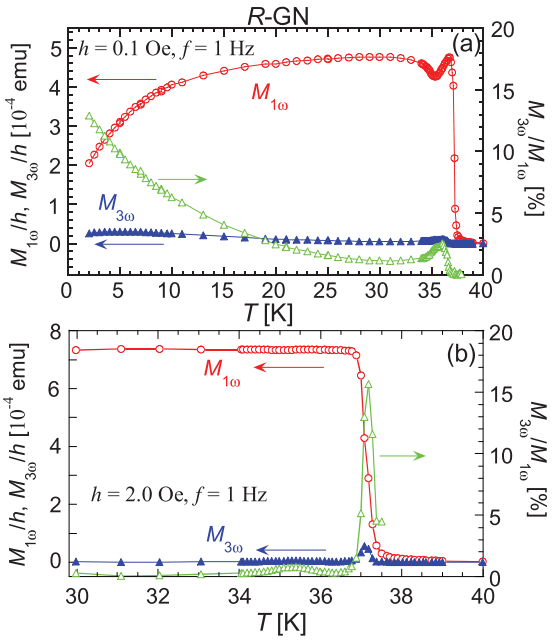

FIG. 6. Temperature dependence in amplitude of both 1ω ($M_{1\omega}/h$) and 3ω ($M_{3\omega}/h$) responses for R-GN, and these ratio ($M_{3\omega}/M_{1\omega}$) at $H_{AC}(f=1$ Hz) for $h=0.1$ Oe and 2.0 Oe. The ac field was applied parallel to the a-axis.

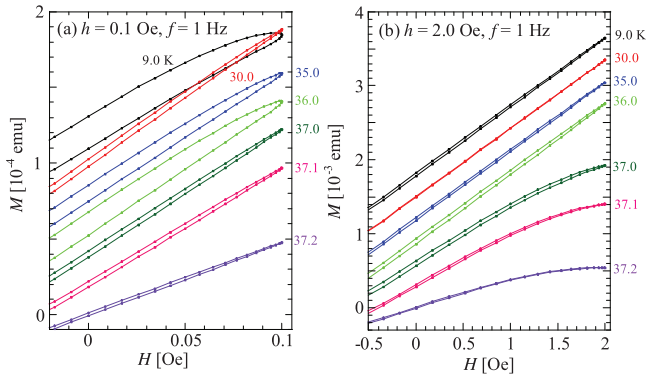

FIG. 7. Magnetic hysteresis under the ac field with $h=0.1$ Oe (a) and 2.0 Oe (b) for R-GN at $f=1$ Hz at some temperatures including characteristic temperatures for **#1**-**#4**: 9.0 K (**#1**), 35.0 K (**#2**), 36.0 K (**#3**), and 37.1 K (**#4**). The magnetic hysteresis was reproduced by summing $M'_{1\omega}$, $M''_{1\omega}$, and $M'_{3\omega}$. For the sake of visual help, the baseline of the vertical axis was shifted every 2×10^{-5} emu in (a) and every 3×10^{-4} emu in (b). The ac field was applied parallel to the a-axis.

and 4. Figure 3 covers the temperature range of 2-45 K, while the temperature range in Fig. 4 is limited to 33-38 K, which corresponds to the solid square in Fig. 3. Here, three features for **#3** and **#4** are identified. First, as can be seen in Figs. 3(b) and 4(c), the $M_{3\omega}$ response for **#4** does not appear at $h=0.1$ Oe, independent of the frequency. Second, the $M_{3\omega}$ response for **#3** exhibits a maximum signal amplitude at around $f=6$ Hz (see Fig. 4(c)). Third, for $f>50$ Hz, the $M_{3\omega}$ response for **#3** disappears, while the corresponding $M''_{1\omega}$ anomaly survives, which suggests that **#3** does not accompany prominent magnetic hysteresis at a high frequency. On the other hand, even at $f=500$ Hz, another **#2** anomaly of the $M_{3\omega}$ response, with reversal of the sign across a critical temperature (T_C), survives, and the **#2** anomaly accompanies a large $M''_{1\omega}$ signal, exhibiting large hysteresis even at a high frequency. This kind of shape of $M'_{3\omega}(T)$ represents a large change in the phase, which reflects the existence of a long-range magnetic order. Indeed, this $M_{3\omega}$ response for **#2** shifts slightly toward the low-temperature side with increasing frequency. In contrast, **#3** appears on the slightly higher-temperature side of **#2**, and disappears for $f>50$ Hz. Thus, **#3** is the ac response due to a small magnetic domain, which can be considered to be the precursor of magnetic ordering (**#2**). In a ferromagnet, $(CH_3NH_3)_2CuCl_2$ with ferromagnetic intralayer interaction, similar $M_{3\omega}$ response as precursor of magnetic ordering was observed.[19] As for **#1**, the f-dependence of $M_{3\omega}$ is smaller than that of the others, and **#1** just shifts toward the higher-temperature side with increasing frequency, as shown in Fig. 3, as in a spin glass phenomenon. Rather, its **#1** response depends on the amplitude of H_{AC}, as shown in Fig. 1, which reveals that it is a weak response to the magnetic field. The results for Figs. 1–4 are discussed again in terms of Figs. 5–7.

VI. DISCUSSION

The characteristic behavior in a series of magnetic anomalies for R-GN is represented in Fig. 5 as a function of f at $h=0.1$ Oe (a) and 2.0 Oe (b). Figure 6 shows the

temperature dependence in amplitude of both the 1ω ($M_{1\omega}/h$) and 3ω ($M_{3\omega}/h$) responses, so that attention is paid to the region of the presence for each harmonic response, and to these ratio ($M_{3\omega}/M_{1\omega}$) at $h=0.1$ Oe (a) and 2.0 Oe (b) for *R*-GN. An overview of the ac magnetic response for *R*-GN from the perspective of a Rayleigh loop is provided in Fig. 7. In the construction of Fig. 5, it is difficult to precisely portray the anomaly position for **#1**. We therefore show only the characteristic region, in which **#1** has a prominent signal, using the temperature of the characteristic peak (which is indicated with *). **#1** was observed in the ac field with h as small as 0.1 Oe, while **#2** and **#3** were observed at both $h=0.1$ and 2.0 Oe. As the frequency increased, **#1**, **#3**, and **#4** all shifted toward the high-temperature side, while **#2** shifted toward the low-temperature side. In particular, **#4** could become gigantic if the ac field were tuned to a large-amplitude, low-frequency field. Figure 6 reveals that at $f=1$ Hz, a high non-linearity appears in such responses as **#1** at $h=0.1$ Oe and **#4** at $h=2.0$ Oe. These responses accompany $M_{3\omega}/M_{1\omega}$ that exceeds 10%, which is much higher than the usual level observed in magnetically glassy systems[15,26,27] and in a helical magnet.[28]

Figure 7 shows how this situation allows prominent magnetic hysteresis in the case of $h=0.1$ and 2.0 Oe at $f=1$ Hz: We provide the magnetic hysteresis obtained at several temperatures including characteristic temperatures for **#1**-**#4**: 9.0 K (**#1**), 35.0 K (**#2**), 36.0 K (**#3**), and 37.1 K (**#4**). Here, the magnetic hysteresis was reproduced by summing three components such as $M'_{1\omega}$, $M''_{1\omega}$, and $M'_{3\omega}$ and thereafter plotting the sum against the magnetic field (H). First, magnetic hysteresis at $h=0.1$ Oe prominently appears at around 9 K and approximately 35-36 K, as shown in Fig. 7(a). Even in the temperature region of 37.0-37.2 K, small hysteresis is seen. All magnetic hysteresis curves seen in Fig. 7(a) indeed originate in the existence of the $M''_{1\omega}$ component. Even at 9.0 K, the ratio of $M''_{1\omega}/M'_{3\omega}$ exceeds 3.0, and the curve is a typical Lissajous curve. Next at $h=2.0$ Oe, as shown in Fig. 7(b), the magnetic hysteresis hardly appears at approximately 30 K, whereas it pronouncedly appears at around 36-37 K. The magnetic hysteresis below 37 K originates in mainly the $M''_{1\omega}$ component, while that for #**4**, observed at around 37.0-37.2 K, is due to the $M'_{3\omega}$ component. In fact, the field dependence of M for #**4** is qualitatively quite different from those below 37 K, suggesting that #**4** appears in the paramagnetic region.

Thus far, we have measured the ac susceptibility of more than ten molecule-based magnets that contain chiral ligands. In some materials, the anomalies of **#2** and **#3** were observed. However, the magnetic anomaly due to **#1**, which accompanied a giant $M_{3\omega}$ response, was observed only in the present *R*-GN and $[Mn\{(R)\text{-pn}\}][Cr(CN)_6][Mn\{(R)\text{-pn}\}_2(H_2O)]_{0.5}(H_2O)_{1.5}$,[33] both of which possess structural chirality, and whose saturation fields in the magnetization curve are both at a level comparable to the amplitude of the ac field. An $M_{3\omega}$ response such as that in **#4**, however, was observed only in *R*-GN. In rac-GN, #**2** and #**3** were observed through the measurement of the polycrystalline sample, whereas **#4** was not detected.[30] According to the Rayleigh law, the appearance of both the out-of-phase component of $M_{1\omega}$ and the in-phase component of $M_{3\omega}$ originates in the magnetic hysteresis in the small ac field. The magnetic responses of **#1**-**#3** were understood as indicating the detection of a normal Rayleigh loop. In the case of **#1**, this suggests that any magnetic fluctuation that survives even below T_C is due to the existence of nonequivalent magnetic sites. Indeed, multiple anomalies appearing below T_C were observed in the spectrum of electron spin resonance, which suggests the formation of a magnetic fine structure below T_C.[34,35] With a large change in the phase of the $M_{3\omega}$ response across a range of temperatures, **#2** then appears. Furthermore, **#2** is quite steady against the change in frequency, so it therefore originates in the magnetic ordering. **#3** is a weak response to the high frequency field, and it reflects a magnetic domain formed over a small space. **#4** is intrinsically different from **#1**-**#3** because the giant $M_{3\omega}$ is accompanied by no energy loss. Furthermore, the characteristic of **#4** is qualitatively different from those of **#1**-**#3** from the perspective of h-dependence of $M_{3\omega}$: $M_{3\omega}$ for **#1**-**#3** was suppressed with increasing h, while that of **#4** was enhanced in that situation. Thus, **#4** is a massless response, unlike the massive response of **#1**-**#3**. Indeed, a neutron diffraction experiment for *R*-GN revealed that in the unit cell, four Mn^{2+} ions and four Cr^{3+} ions change the direction of the magnetic moment every ninety degrees against the a-axis, and the magnetic chirality closed within the unit cell is present.[36] The magnetic structure is commensurate, while there is a modulated spin structure in the unit cell. As mentioned above, **#4** has not been observed in the racemic system.[30] We consider that the development of a free degree of magnetic chirality at a temperature just above T_C is what produced **#4**.

VII. CONCLUSION

Complex nonlinear magnetic responses were investigated in the molecule-based magnet *R*-GN, in which single-handed chiral ligands construct a molecular network with structural chirality, by means of the diagnostics of the magnetic hysteresis that mainly uses the third-harmonic magnetic response. Four kinds of nonlinear magnetic responses were observed; from high-temperature side, they are: (**#4**) in the paramagnetic region, (**#3**) just above magnetic ordering, (**#2**) on magnetic ordering, and (**#1**) on a sufficiently low-temperature side of magnetic ordering. The $M_{3\omega}$ signal of **#1**-**#3** was suppressed with increasing the amplitude of the ac field, while that of **#4** was enhanced in the same situation. The nonlinear magnetic responses of **#1**-**#3** are understood to indicate the detection of a normal Rayleigh loop. **#1** reveals that the magnetic fluctuation that appears in a small oscillating field survives below the magnetic ordering temperature. **#2** originates in the magnetic ordering. **#3** reflects the formation of a small magnetic domain. **#4** represents an intrinsically different response from **#1**-**#3**, and reflects the development of a free degree of magnetic chirality in the paramagnetic region. Through the ac magnetic susceptibility measurements, we acquired important knowledge on magnetic domain formation at the low field limit that could not be obtained via the magnetic hysteresis in the large dc magnetic field.

ACKNOWLEDGMENTS

This work was supported by a Grant-in-Aid for Scientific Research (A) (No. 18205023) from the Ministry of Education, Culture, Sports, Science and Technology (MEXT), Japan.

[1]C. Train, M. Gruselle, and M. Verdaguer, Chem. Soc. Rev. **40**, 3297 (2011).
[2]H. Kumagai and K. Inoue, Angew. Chem., Int. Ed. **38**, 1601 (1999).
[3]K. Inoue, K. Kikuchi, M. Ohba, and H. Okawa, Angew. Chem., Int. Ed. **42**, 4810 (2003).
[4]K. Ikeda, S. Ohkoshi, and K. Hashimoto, J. Appl. Phys. **93**, 1371 (2003).
[5]T. Nuida, T. Matsuda, H. Tokoro, S. Sakurai, K. Hashimoto, and S. Ohkoshi, J. Am. Chem. Soc. **127**, 11604 (2005).
[6]C. Train, T. Nuida, R. Gheorghe, M. Gruselle, and S. Ohkoshi, J. Am. Chem. Soc. **131**, 16838 (2009).
[7]G. L. J. A. Rikken and E. Raupach, Nature **390**, 493 (1997).
[8]G. L. J. A. Rikken and E. Raupach, Phys. Rev. E **58**, 5081 (1998).
[9]G. L. J. A. Rikken, C. Strohm, and P. Wyder, Phys. Rev. Lett. **89**, 133005 (2002).
[10]C. Train, R. Gheorghe, V. Krstic, L. M. Chamoreau, N. S. Ovanesyan, G. L. J. A. Rikken, M. Gruselle, and M. Verdaguer, Nature Mater. **7**, 729 (2008).
[11]M. Fiebig, D. Fröhlich, B. B. Krichevtsov, and R. V. Pisarev, Phys. Rev. Lett. **73**, 2127 (1994).
[12]M. Fiebig, D. Fröhlich, G. Sluyterman, and R. V. Pisarev, Appl. Phys. Lett. **66**, 2906 (1995).
[13]V. N. Muthukumar, R. Valentí, and C. Gros, Phys. Rev. B **54**, 433 (1996).
[14]J. A. Mydosh, *Spin Glasses: An Experimental Introduction* (Taylor & Francis, London, 1993).
[15]M. Suzuki, Prog. Theor. Phys. **58**, 1151 (1977).
[16]Y. Miyako, S. Shikazawa, T. Saito, and Y. G. Yuochunas, J. Phys. Soc. Jpn. **46**, 1951 (1979).
[17]S. Fujiki and S. Katsura, Prog. Theor. Phys. **65**, 1130 (1981).
[18]T. Satō and Y. Miyako, J. Phys. Soc. Jpn. **51**, 1394 (1981).
[19]N. Narita and I. Yamada, J. Phys. Soc. Jpn. **65**, 4054 (1996).
[20]M. A. Gîrtu, C. M. Wynn, W. Fujita, K. Awaga, and A. J. Epstein, Phys. Rev. B **57**, R11058 (1998).
[21]M. Mito, M. Ogawa, H. Deguchi, M. Yamashita, and H. Miyasaka, J. Appl. Phys. **107**, 124316 (2010).
[22]L. Rayleigh, Philos. Mag. **23**, 225 (1887).
[23]F. Milstein, J. A. Baldwin, Jr., and M. Rizzuto, J. Appl. Phys. **46**, 4002 (1975).
[24]J. A. Baldwin, Jr., J. Revol, and F. Milstein, Phys. Rev. B **15**, 426 (1977).
[25]T. Shirane, T. Bitoh, and S. Chikazawa, J. Korean Phys. Soc. **46**, 694 (2005).
[26]G. H. J. Wantenaar, S. J. Campbell, D. H. Chaplin, T. J. McKenna, and G. V. H. Wilson, J. Appl. Phys. **57**, 471 (1985).
[27]R. Becker and W. Döring, *Ferromagnetismus* (Springer, Berlin, 1939).
[28]M. Mito, K. Iriguchi, Y. Taniguchi, M. Kawase, S. Takagi, and H. Deguchi, J. Phys. Soc. Jpn. **80**, 064707 (2011).
[29]Y. Yoshida, K. Inoue, and M. Kurmoo, Chem. Lett. **37**, 586 (2008).
[30]M. Mito, K. Iriguchi, H. Deguchi, J. Kishine, K. Kikuchi, H. Osumi, Y. Yoshida, and K. Inoue, Phys. Rev. B **79**, 012406 (2009).
[31]K. Iriguchi, Y. Komorida, I. Akiyama, M. Mito, J. Kishine, H. Deguchi, Y. Yoshida, and K. Inoue, J. Phys. Soc. Jpn. **79**(Suppl A), 192 (2007).
[32]K. Tsuruta, M. Mito, H. Deguchi, S. Takagi, Y. Yoshida, and K. Inoue, Polyhedron **30**, 3262 (2011).
[33]K. Inoue, H. Imai, P. S. Ghalsasi, K. Kikuchi, M. Ohba, and H. Okawa, Angew. Chem., Int. Ed. **113**, 4372 (2001).
[34]R. B. Morgunov, V. L. Berdinskii, M. V. Kirman, K. Inoue, J. Kishine, Y. Yoshida, and Y. Tanimoto, JETP Lett. **84**, 446 (2006).
[35]R. B. Morgunov, M. V. Kirman, K. Inoue, Y. Tanimoto, J. Kishine, A. S. Ovchinnikov, and O. Kazakova, Phys. Rev. B **77**, 184419 (2008).
[36]C. Gonzalez, J. Campo, G. J. McIntyre, F. Palacio, Y. Numata, Y. Yoshida, K. Kikuchi, and K. Inoue (unpublished).